Jour. Fac. Sci., Hokkaido Univ., Ser. VII (Geophysics), Vol. 7, No. 3, 257–267, 1983.

A New Method of Measuring in-situ Stress

Itaru Maeda

*Research Center for Earthquake Prediction, Faculty of Science,
Hokkaido University, Sapporo 060, Japan*

and

Nobuyuki Shimizu

*Department of Geophysics, Faculty of Science,
Hokkaido University, Sapporo 060, Japan*

(Received October 30, 1982)

Abstract

A new method of measuring in-situ stress was presented. The method is based on the anisotropic behavior of sound wave velocity in rocks under non-hydrostatic stress. It comprises four procedures; 1) drilling small holes into a bottom rock of a borehole, 2) measuring the sound velocities in the bottom rock in many directions, 3) measuring the velocities of the core sample as a function of stress, and 4) comparing the velocities obtained by 2) and 3). A device to execute 1) and 2) was designed. We simulated these procedures by a room experiment under a uniaxial stress condition and examined the capability of this method. We can apply this method when a stress acting on a rock is less than a certain value over which the anisotropy by compaction becomes negligible or constant.

1. Introduction

There are several methods of measuring in-situ stress of rock basement. These methods have been extensively used to measure the crustal stress for earthquake prediction: Ikeda et al. (1981) measured the stress by the hydraulic fracture method, and Tanaka et al. (1980) used the stress release method to measure the stress in the western Japan. Although these methods have given some plausible values for stress, because they are based on some kinds of theories and assumptions (as examples, elastic theory for isotropic medium, and that one of the principal axes of stress coincides with the borehole axis), the stresses obtained by these methods are not always reliable. It is necessary, therefore, to develop another method which is based on intrinsically different principles from others to get more reliable stresses. A method which has no assumption and is not based on theories is more desirable to measure the in-situ stress of the crust.

A purpose of the present paper is to demonstrate a new method of measuring stress. We will show, first, an idea of the method, then, give a procedure and a device to accomplish the idea. We will give a test result of the method in a case of rock sample being subject to uniaxial stress.

2. Principle

Anisotropic behavior of sound velocity in rocks under nonhydrostatic stress is well known (e.g. Tocher, 1957). Typical variation of the velocity, V, versus differential stress, σ, under low or no confining pressure is shown in Fig. 1(a). The velocity of sound propagating parallel to the stress axis shows largest increase up to a stress, σ_T. On the other hand, the sound propagating perpendicular to the stress axis shows largest decrease over a stress, σ_D, which is identified as the dilatancy onset stress. Variation of the velocity anisotropy versus differential stress is shown in Fig. 1(b) (Shimizu, 1983). There may be many ways to define magnitude of the anisotropy. In this study, we define the magnitude of the velocity anisotropy, Va, as

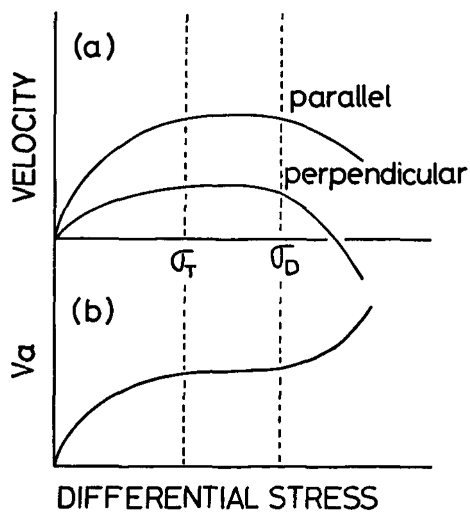

Fig. 1 (a) Typical variation of velocities of sound waves propagating parallel and perpendicular to the stress axis and (b) that of the velocity anisotropy, Va, versus differential stress.

$$V_a(\sigma) = 2\frac{V_{\max}(\sigma) - V_{\min}(\sigma)}{V_{\max}(\sigma) + V_{\min}(\sigma)}$$

where $V_{\max}(\sigma)$ and $V_{\min}(\sigma)$ are a maximum and a minimum velocity at a stress, σ, respectively. Knowing the velocity anisotropy of a rock sample, we can deduce the stress condition acted on the sample but accuracy of the stress so obtained depends on the stress actually acted on the sample. As can be seen from Fig. 1(b), the accuracy of the velocity so obtained is proportional to the tangent of the velocity anisotropy curve; under a stress between σ_T and σ_D, stress so deduced is unreliable.

The Va depends on rock species, presence of water, and magnitude of the confining pressure. Since the presence of water reduces the velocity change by differential stress (Nur and Simmons, 1969), it may reduce Va. The confining pressure also reduces Va (Shimizu, 1983). Over a certain confining pressure, Va becomes negligible under a differential stress below σ_D. Reduction of Va means that the accuracy of the stress deduced from Va becomes low. Directions of the principal axes of the stress field deduced from the pattern of the velocity anisotropy are affected by not only the above factors but also by intrinsic anisotropy which does not depend on stress.

3. Procedure

In this section we consider a procedure to apply the principle stated in a general three dimensional stress condition. We assume that a wave front of sound emitted from a point and propagating through a rock body, forms an ellipsoidal surface. To express the ellipsoid, we make some definitions. Let the sizes of the three principal axes of the ellipsoid be $a\cdot t$, $b\cdot t$, and $c\cdot t$, where t is time and a, b, and c are velocities of the sound waves propagating in the principal directions. We call the ellipsoid at $t=1$ the velocity ellipsoid. We call a coordinate system whose axes coincide with that of the ellipsoid the X'-system. We consider the other coordinate system X whose origin coincides with that of X'.

Let a vector r_i in X be transformed by an operation $\boldsymbol{M}$ to $\boldsymbol{r}_i'$ in X' i.e.

$$\boldsymbol{r}_i' = \boldsymbol{M}\boldsymbol{r}_i \qquad i = 1,\cdots,n$$

$$\boldsymbol{r}_i' = (x_i', y_i', z_i')$$

$$\boldsymbol{r}_i = (x_i, y_i, z_i) = \boldsymbol{r}_i(r_i, \theta_i, \varphi_i)$$

$$M=\begin{pmatrix} \cos\varphi\cos\psi-\sin\varphi\cos\theta\sin\psi, & \cos\varphi\sin\psi+\sin\varphi\cos\theta\cos\psi, & \sin\varphi\sin\theta \\ -\sin\varphi\cos\psi-\cos\varphi\cos\theta\sin\psi, & -\sin\varphi\sin\psi+\cos\varphi\cos\theta\cos\psi, & \cos\varphi\sin\theta \\ \sin\theta\sin\psi, & -\sin\theta\cos\psi, & \cos\theta \end{pmatrix}$$

where θ, φ, and ψ, are the Euler angles of X' measured from X. By definition, r_i' satisfies an equation of the velocity ellipsoid:

$$\left(\frac{x'}{a}\right)^2+\left(\frac{y'}{b}\right)^2+\left(\frac{z'}{c}\right)^2=1$$

Let r_i be the sound velocity propagating in a direction (θ_i, φ_i) of the X-system. If we have n velocities, we obtain n equations with six unknown variables, a, b, c, θ, φ, and ψ. The number n must be greater than six to be able to solve the equations. If we measure velocities in more than six directions in the field, we can obtain directions of the principal stresses in terms of θ, φ, and ψ, because the directions of the principal velocities correspond to those of the stresses. Next, if we can get a core sample of the rock in which the field-measurement was made, we can obtain values for the principal stresses acting in the field by the following method. By compressing the sample in a triaxial press from the directions obtained in the field measurement, we can find the stress when the sound velocity measured during compression fits that obtained in the field-measurement.

4. Design

We will show a possible design of a device that makes it possible to apply the method stated to an actual field-measurement in a borehole. The device must satisfy the following conditions.

(1) The diameter of the device is less than 150 mm.

(2) The device has as many sensors as possible. The 'sensor' means that it is used as both an emitter and receiver of sound waves. The number of independent directions of sound propagation (path direction) among all combinations of any two sensors, must be greater than six. This means that the number of the sensors should be greater than four.

(3) The sensors must be distributed three dimensionally.

To satisfy condition (3), we propose to drill small diameter holes (we call these holes sensor holes) into the bottom of the borehole (Fig. 2). After drilling the sensor holes, rods with sensors attached on the ends must be inserted into them. We designed a device to achieve this operation. The

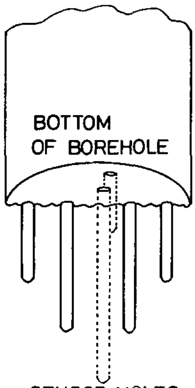

Fig. 2 Sensor holes drilled into a bottom of a borehole.

Fig. 3 Vertical section of the device. →

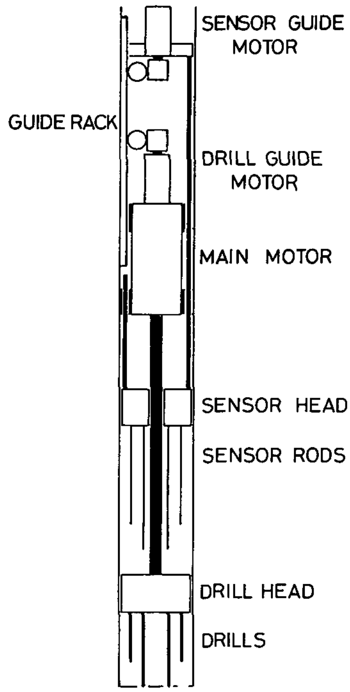

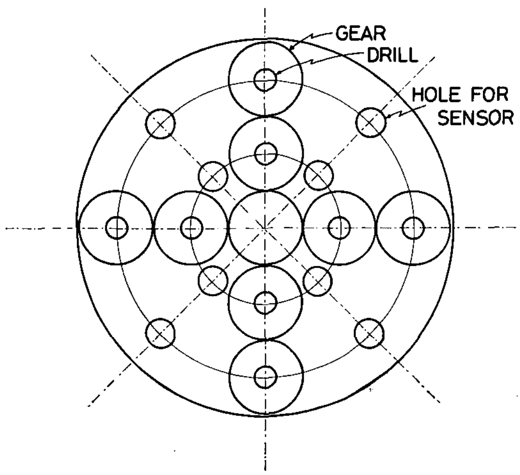

Fig. 4 Gear pattern of the drill head shown in Fig. 3. After drilling, we rotate the drill head 45° and insert the sensor rods attached to the drill head, passing through the holes of the head, to the sensor holes.

device is shown schematically in Fig. 3. Fig. 4 shows the gear pattern in the drill head. The center gear is connected to the power rod from the motor, and the other gears are attached to drill bits. This pattern makes it possible for the number of the sensors to be eight and the number of path directions to be twenty-eight. This pattern satisfies condition (2).

After assuming that the sensor rods having a diameter of 5–8 mm can pass through the drill head, there remains little leeway for changing the pattern. We can adjust the size of the gear to satisfy condition (1).

5. Test experiment

We now test the principle and the procedure to obtain stress under uniaxial compressive stress. We prepared two granite samples from a rock outcrop. One sample having a size of $31\times31\times95\ \text{mm}^3$ was used to obtain velocities as a function of the axial stress in several directions using the usual sound transmission method in which the sensors were attached on the surface of the sample. Fig. 5 shows the velocity changes which were smoothed in four directions.

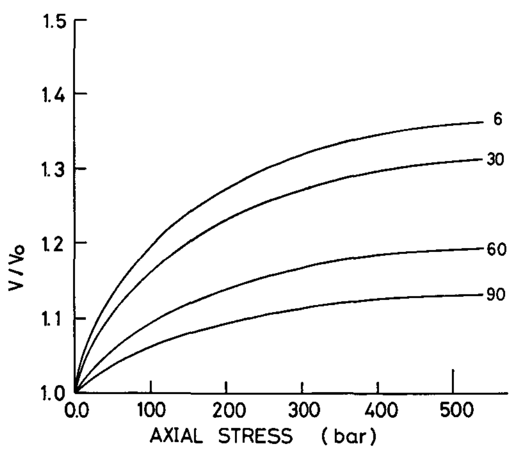

Fig. 5 Velocity changes divided by the initial ones versus axial stress. Values attached to curves indicate the path directions against the stress axis.

The other sample had a larger size of $300\times300\times800\ \text{mm}^3$ permitting sensors with actual distribution size and pattern to be implanted into the sample. We drilled eight sensor holes into the large sample with a distribution

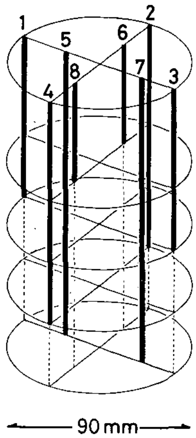

←Fig. 6 Actual sensor hole pattern drilled into the sample rock. The number attached to each hole corresponds to the sensor number in Fig.'s 7 and 9 and Tables 1 and 2.

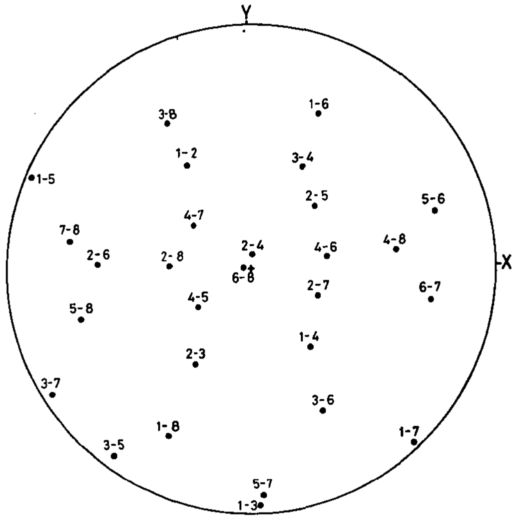

Fig. 7 Path directions of the present experiment plotted in the Wulff's net. The numbers in the form of (*m*-*n*) means that sound emitted from *m*-th sensor is received at *n*-th sensor. Center cross is the direction of the stress axis.

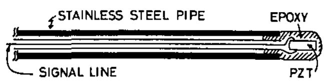

Fig. 8 Structure of a sensor rod.

pattern as shown in Fig. 6. This distribution makes it possible to distribute the path directions nearly uniformly over a solid angle 4π (Fig. 7). The structure of the sensor is shown in Fig. 8. The sensor rods were joined by their inner ends to the hole bottoms with Epoxy resin. It is not clear whether such a method to affix the sensors can be applied in actual field situations.

Table 1 shows the relative emitter- receiver position over possible combinations of the sensors. P-wave velocities between sensors at several axial

Table 1. Relative positions between sensors.

R\S	1	2	3	4	5	6	7	8
1	D	69.1	89.5	70.4	58.4	52.3	79.8	54.7
	θ	52.6	92.5	136.8	89.1	68.7	91.4	116.3
	Φ	−30.7	−1.6	−37.0	−66.5	24.7	−43.1	27.2
2			67.4	93.7	54.0	53.7	52.5	83.3
			133.0	174.6	139.6	115.4	146.9	142.6
			31.1	186.6	226.9	93.4	−67.3	94.1
3				74.4	83.6	55.5	60.6	55.9
				129.6	86.7	65.6	88.2	111.3
				−152.5	−142.3	153.1	−120.9	151.5
4					59.6	86.1	58.9	58.3
					28.9	35.3	33.2	62.3
					−121.8	83.3	−52.2	84.3
5						78.9	35.1	82.5
						76.7	94.7	107.7
						74.1	−1.6	75.0
6							79.0	43.3
							105.4	177.2
							−79.4	109.3
7								81.4
								105.8
								100.8

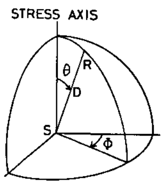

stresses are listed in Table 2. There is a large scattering in the measured values. One cause is the inhomogeneity of the sample in a dimension of several centimeters. There may be other unknown factors.

Fig. 9 shows the Va patterns at given axial stresses on the Wulff's stereographic net. In each figure, the center is the direction of the stress axis. We can easily identify the stress axis from the figure at each stress with the accuracy of $\pm 10°$, which is sufficient at present. Contours of equi-velocity increase divided by velocities at zero stress should be concentric circles but they are not in the present case. As a result, there seems to be a second axis of stress which does not really exist. It is expected, nevertheless, that at least the direction of the maximum principal stress can be detected.

We can obtain 'stress' comparing the normalized increases of the velocities at given stresses in Fig. 9 with the ones in Fig. 5. We call the 'stress' so obtained the observed stress. Table 3 gives the given stresses and the observed stresses. The observed stresses were obtained by two methods; one by comparing the maximum velocity increases in Fig. 5 with that in Fig. 9, the other by comparing the Va's presented in the both figures. The accuracy was within 1.5 figures.

Table 2. Measured velocities between sensors at five stresses.

0 bar

	2	3	4	5	6	7	8
1	4.06	4.07	3.83	3.24	3.90	3.71	3.51
2		4.06	4.36	3.65	4.40	3.80	4.06
3			3.82	3.98	4.34	4.21	4.44
4				4.20	4.20	4.33	4.05
5					3.87	3.08	3.51
6						4.16	4.01
7							4.07

35 bars

	2	3	4	5	6	7	8
1	4.43	4.07	4.05	3.44	4.22	3.89	3.51
2		4.21	4.88	3.97	4.55	4.01	4.48
3			4.09	4.08	4.63	4.33	3.94
4				4.52	4.58	4.60	4.11
5					4.03	3.13	3.84
6						4.25	4.51
7							4.24

133 bars

	2	3	4	5	6	7	8
1	4.67	4.26	4.19	3.65	4.29	3.95	3.70
2		4.38	5.21	4.15	4.63	4.45	4.68
3			4.18	4.14	4.70	4.81	4.74
4				4.66	4.89	4.91	4.22
5					4.15	3.19	3.93
6						4.34	4.81
7							4.42

206 bars

	2	3	4	5	6	7	8
1	4.87	4.48	4.29	3.74	4.36	3.99	4.02
2		4.49	5.45	4.29	4.79	4.61	4.84
3			4.33	4.18	4.78	4.59	4.82
4				4.89	5.06	4.99	4.29
5					4.24	3.25	4.02
6						4.44	5.03
7							4.42

296 bars

	2	3	4	5	6	7	8
1	4.94	4.48	4.29	3.84	4.43	4.03	4.08
2		4.55	5.58	4.35	4.88	4.61	4.84
3			4.38	4.29	4.87	4.66	4.90
4				4.89	5.25	5.08	4.29
5					4.34	3.25	4.02
6						4.54	5.15
7							4.42

VELOCITIES (km/sec.)

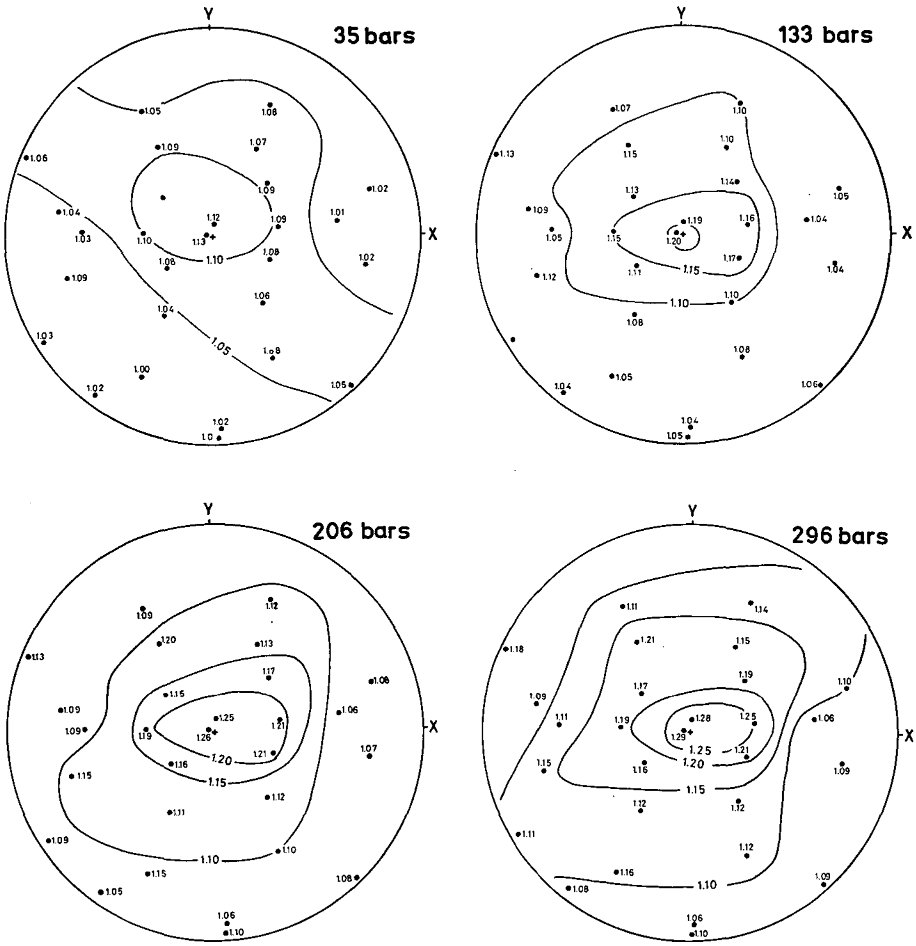

Fig. 9 Velocity anisotropy patterns at assigned stresses. The number attached to each direction is the amount of the velocity change divided by the initial velocity.

Table 3. Given stresses and observed stresses obtained by two methods; for V_{max}, the stresses are deduced by comparing the maximum values in Fig. 9 and the upper most curve in Fig. 5, and for Va, they are deduced from Va's in Fig. 5 and Fig. 9.

GIVEN	STRESS (bars (%))	
	V_{max}	Va
35	40 (+14)	40 (+14)
133	95 (−29)	85 (−34)
206	170 (−17)	170 (−17)
296	230 (−22)	210 (−29)

6. Conclusion

We have proposed a new method to measure in-situ stress in boreholes. The principle of the method is to use the anisotropic behavior of sound wave velocity in rocks under nonhydrostatic stress. The basic design of a device to achieve the measurement has been given.

We tested the method according to the procedure in a case of low uniaxial stress condition. The direction of the maximum principal stress (stress axis) could be obtained with sufficient accuracy. The accuracy of the observed stresses was within 1.5 figures. It has been considered that reliability of results depends on rock species, water content, differences between a cored sample and a rock in which a field measurement was made, and confining pressure. In other words, applicability of the present method is limited to rocks which have 'good nature' about the anisotropic behavior of sound waves. If the stress acting on the crust is higher than a certain stress, σ_T, over which Va becomes almost constant, the present method is not applicable.

References

Ikeda, R. and H. Takahashi, 1981. Stress measurement by hydrofracturing at Futtsu city, Chiba prefecture (in Japanese), Zisin, **34**, 565–576

Nur, A. and G. Simmons, 1969. The effect of saturation on velocity in low porosity rocks, Earth Planet. Sci. Lett., **7**, 183–193

Shimizu, N., 1983. in preparation

Tanaka, Y., I. Oka, T. Saito, S. Yanagitani, S. Matsushima, H. Yukutake, K. Mikumo, K. Oike, and K. Hujimori, 1980. Basic research for measurement of the crustal stress and its variation (in Japanese), Rep. Nat. Sci. Found. Grant 346041, pp 25

Tocher, D., 1957. Anisotropy in rocks under simple compression, EOS Trans. AGU, **38**, 89–94